Preparation of $SrVO_3/SrTiO_3$ (001) Epitaxial Thin Films by Pulse Laser Deposition

August 17, 2022

Tina Tong[1]
Student ID: 912529878

Mentor: Dr. Ambrose Seo

[1] *Department of Physics and Astronomy*
University of Kentucky
Lexington, KY 40506, USA

Abstract

Strontium vanadate, $SrVO_3$ (SVO), is a cubic perovskite that exhibits highly conductive behavior making it a candidate as a transparent conducting oxide (TCO). Furthermore, $SrVO_3$ being a highly correlated material means that when it is doped or reduced in dimensionality, it undergoes metal-insulator transition (MIT), this property makes $SrVO_3$ of great interest to research. This experiment aims at synthesizing a $SrVO_3$/ $SrTiO_3$ epitaxial thin film by Pulse Laser Deposition (PLD) using $Sr_2V_2O_7$ as the target and $SrTiO_3$ (001) as the substrate. While the deposition was successful, the quality of the thin film was deemed poor due to the presence of additional $SrVO_3$ secondary peaks.

1 Introduction

A perovskite refers to any material with the crystal structure following the formula ABX_3 [1], and these perovskites are of great interest as result of the strange new properties that are exhibited like ferroelectricity, superconductivity, etc.. For example, when $LaAlO_3$ is grown on $SrTiO_3$, these two non-conductive materials display conductive behavior.

The word transparent conducting oxide (TCO) refers to electrically conductive materials that have high optical transmission at visible wavelengths. These materials are typically doped metal oxides and what makes them effective is the low resistivity and high transmittance properties that they have [1]. These transparent conducting oxides tend to be used in solar cells, displays, onto-electrical interfaces, etc.. It is worth mentioning, that despite the extensive uses transparent conducting oxides have, they are fragile and break down with use.

Strontium vanadate is a perovskite that has been the topic of research for condensed matter physics due to it being a strongly correlated material and having a low work function. $SrVO_3$ being a strongly correlated material, when $SrVO_3$ is doped or reduced in dimensionality, it undergoes metal-insulator transition [2,3,4]. Even more so, having been discovered that $SrVO_3$ has high transmittance and low resistivity, it has also been considered as a candidate as a transparent conducting oxide (TCO) this refers to materials used in screen displays or solar cells [1]. This is particularly important considering the industry standard, Indium Tin Oxide (ITO), is extremely limited in its amount and therefore, extremely expensive. The intention of this project is to successfully synthesize $SrVO_3$ on $SrTiO_3$ using a $Sr_2V_2O_7$ target [5].

2 Procedure

2.1 Preparing the Target

The chemical reaction for $Sr_2V_2O_7$:

$$2SrCO_3 + V_2O_5 \rightarrow Sr_2V_2O_7 + 2CO_2$$

The sample $Sr_2V_2O_7$ was prepared first by using $SrCO_3$ and V_2O_5 powders. For each of the starting materials, X-Ray Diffraction was done to ensure purity and to confirm the powders were not unknowingly contaminated, refer to Figure 1.

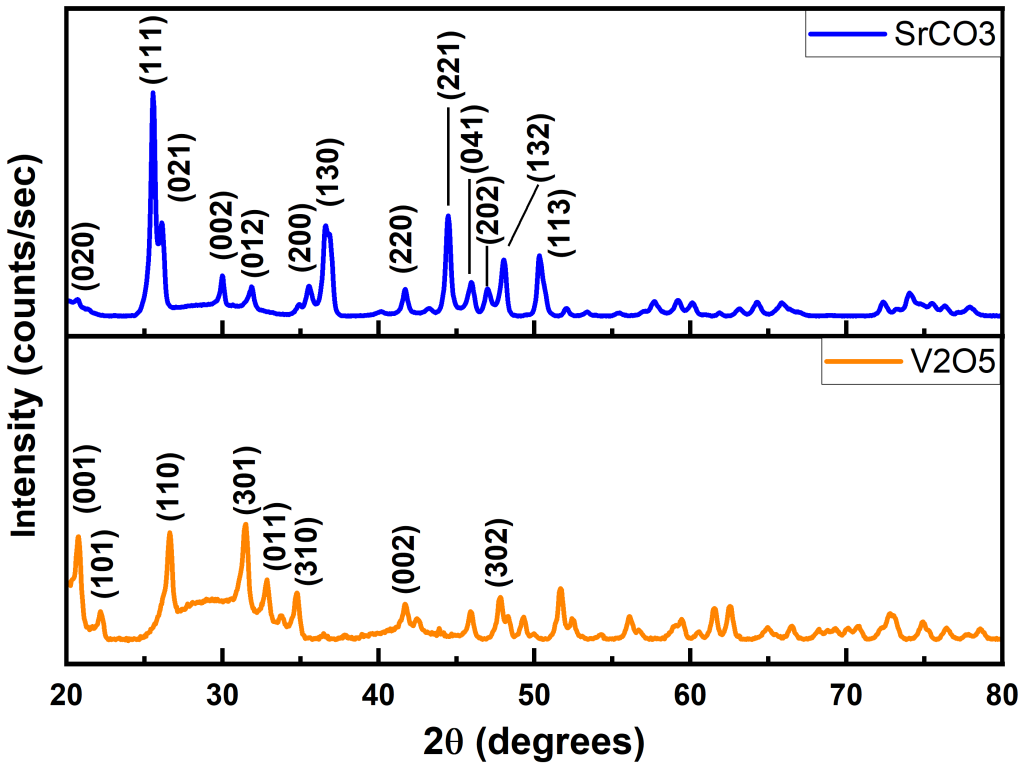

Figure 1: XRD graphs of $SrCO_3$ and V_2O_5 powders

Using the balanced equation, it was determined that to synthesize approximately 1 gram of $Sr_2V_2O_7$, 0.759 grams of $SrCO_3$ and 0.467 grams of V_2O_5 were required. It should be noted that the balanced used to weight each of the reactants was not working properly resulting in a ± 0.05 grams for each measurement. The stoichiometric amounts of the reactants were grounded using a motor and pestle until fine, the molar ratio being 2:1 [6,7]. From there, the resulting mixture was transferred to an alumina crucible and heated to 1000 °C for 24 hours in air in a furnace to calcine, ramping up to 1000 °C in 4 hours and ramping down by letting the furnace naturally cool until it reached room temperature. This was done to remove any carbon in the mixture. The powder pre-calcination was a yellow color, as seen in Figure 2, indicating a small band gap whereas the powder post-calcination was a blue-white color, as seen in Figure 3, indicating a large band gap.

Figure 2: Powder pre-calcination

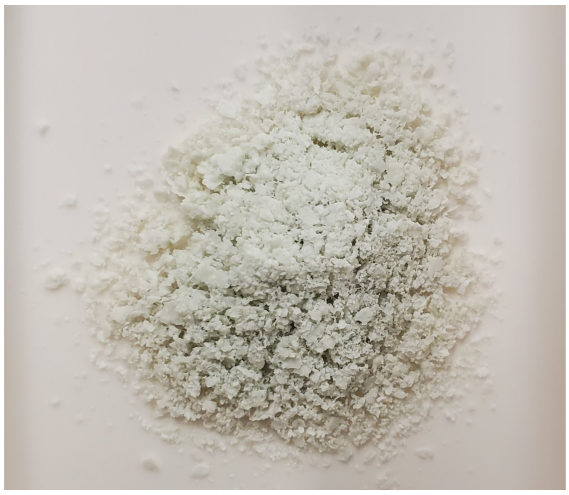

Figure 3: Powder post-calcination

The process of regrinding and reheating the homogeneously mixed powder was repeating until only $Sr_2V_2O_7$ was present as observed through Powder X-Ray Diffraction (PXRD). In many other experiments where $Sr_2V_2O_7$ was synthesized, the process was repeated, but in this experiment, it was found that repeating would be unnecessary despite the $Sr_2V_2O_7$ powder still retaining the secondary phase $Sr_3V_2O_7$. This additional phase was not concerning due to the presence of it being few and there having been other experiments conducted using 85% $SrVO_3$ and 15% of a secondary phase [7]. While, there is a method to synthesize $SrVO_3$ from $Sr_2V_2O_7$, in this experiment only $Sr_2V_2O_7$ was synthesized and used as the target for Pulse Laser Deposition (PLD).

The steps are fairly similar, the only difference being that the $SrVO_3$ requires $Sr_2V_2O_7$ to be heated in a furnace under gas flow of 95% Argon to 5% Hydrogen. $SrVO_3$ was not created in this experiment due to not having the gas and not having a working gas flowing furnace.

Figure 4: Pellet die

Figure 5: Pellet press

The calcined powder was reground and was then molded into a 2mm diameter pellet using a dry pellet pressing die, as shown by Figure 4. The pellet die provided shapes the powder into a pellet, where it is then put under 21 tons of pressure using a hydraulic press, refer to Figure 5 for 1 hour.

Figure 6: Pellet pre-sinter

Figure 7: Pellet post-sinter

Once the pellet has been successfully formed as shown in Figure 6, it is sintered at 1000 °C for 24 hours using the same ramping up and down conditions as the calcination process. XRD should be performed on the sintered pellet to report any changes and determine if the pellet is still $Sr_2V_2O_7$. Figure 7 shows the sintered pellet; the white peaks may indicate the powder may not have been

ground enough.

2.2 Preparing the Substrate

The processes used to prepare the substrate were deionized water leeching and thermal annealing. These processes were crucial to achieving an atomically flat surface of a substrate in order to prepare a well characterized sample and to exhibit interesting properties [8]. The substrate used in this experiment was $SrTiO_3$, this substrate was chosen based on the compatibility between the crystal structures of $SrTiO_3$ and $SrVO_3$, that being both are cubic, and due to multiple other experiments having used $SrTiO_3$ as the substrate to grow the $SrVO_3$ thin film. To perform the water leeching, $SrTiO_3$ was rinsed in deionized water by agitating it for approximately 30 seconds at room temperature, and, subsequently, was dried using air. Following after the water leeching, the thermal annealing process was done. This process involves heating the substrate in a furnace at 1000 °C for 1 hour. There were 5 $SrTiO_3$ samples used and for each, the water leeching, and annealing was preformed twice, where the sample yielding the best result was chosen.

Figure 8: $SrTiO_3$ substrates before 1^{st} water leeching and annealing

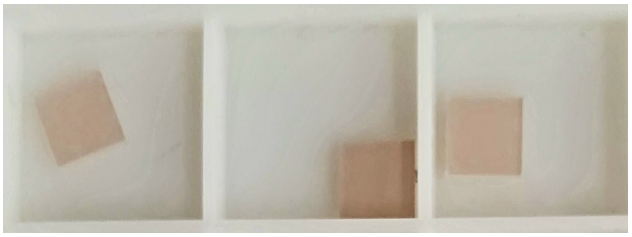

Figure 9: $SrTiO_3$ substrates after 1^{st} water leeching and annealing

As seen by Figures 8 and 9 there is a slight change in color, but overall on a macroscopic level, any other changes are unnoticeable. The surface was characterized after each water leeching and annealing process using an atomic force microscope (AFM). Figures 10 and 11 display the AFM topography of $SrTiO_3$ substrate after the first deionized-water leeching and thermal annealing process with the line profile, where the step height is 3.9 Å.

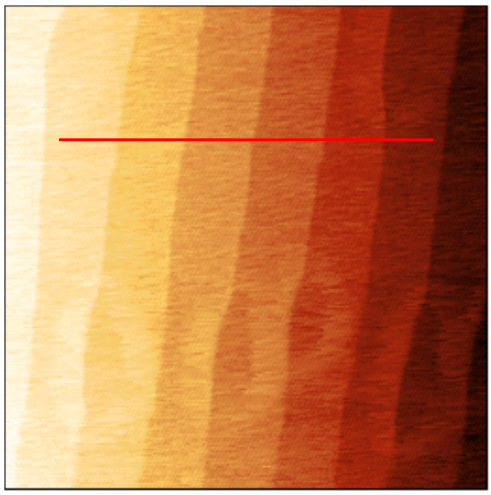

Figure 10: AFM topography of $SrTiO_3$ substrate after 1^{st} water leeching and annealing

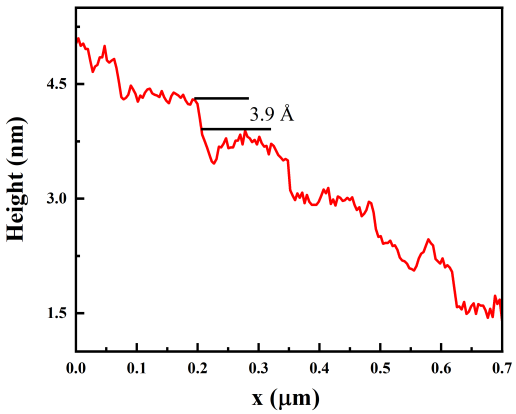

Figure 11: The line profile of the AFM topography

3 Data and Methods

3.1 X-Ray Diffraction (XRD)

XRD refers to the scattering of x-rays as a result of hitting the atoms of a crystal. The crystals can be thought of as a regular array of atoms and the x-rays as waves. When an x-ray hits an electron, this creates secondary circular waves from the electron. Most waves created are destroyed by destructive waves, while others are amplified by constructive waves. The effects of these wave interference increases due to the cumulative effect of reflection in successive crystallographic planes

of the crystalline lattice. Figure 12 provides a XRD diagram and Figure 13 shows the XRD machine used.

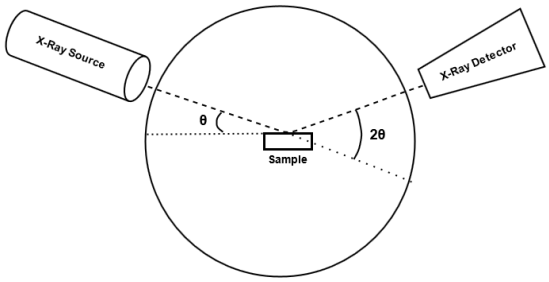

Figure 12: XRD diagram

Figure 13: XRD machine

XRD allows for us to determine the crystal structure, purity, and its current phase; for our experiment, this became extremely important due to $SrVO_3$ having several secondary phases like $Sr_2V_2O_7$ and $Sr_3V_2O_8$. One main concern for using $Sr_2V_2O_7$ as the target for PLD was the crystal structure. $Sr_2V_2O_7$ is triclinic meaning that each length of the crystal is unequal and the angles between them are also different making this crystal extremely unsymmetrical which results in the numerous peaks as seen in Figure . Whereas $SrVO_3$ has a cubic crystal structure, meaning each of the lengths are equal and the angles are all 90°, which is what makes it symmetrical and have relatively fewer peaks compared to $Sr_2V_2O_7$. Furthermore, having fewer, distinct peaks makes characterizing the XRD graphs simpler to observe if there are any additional secondary phases.

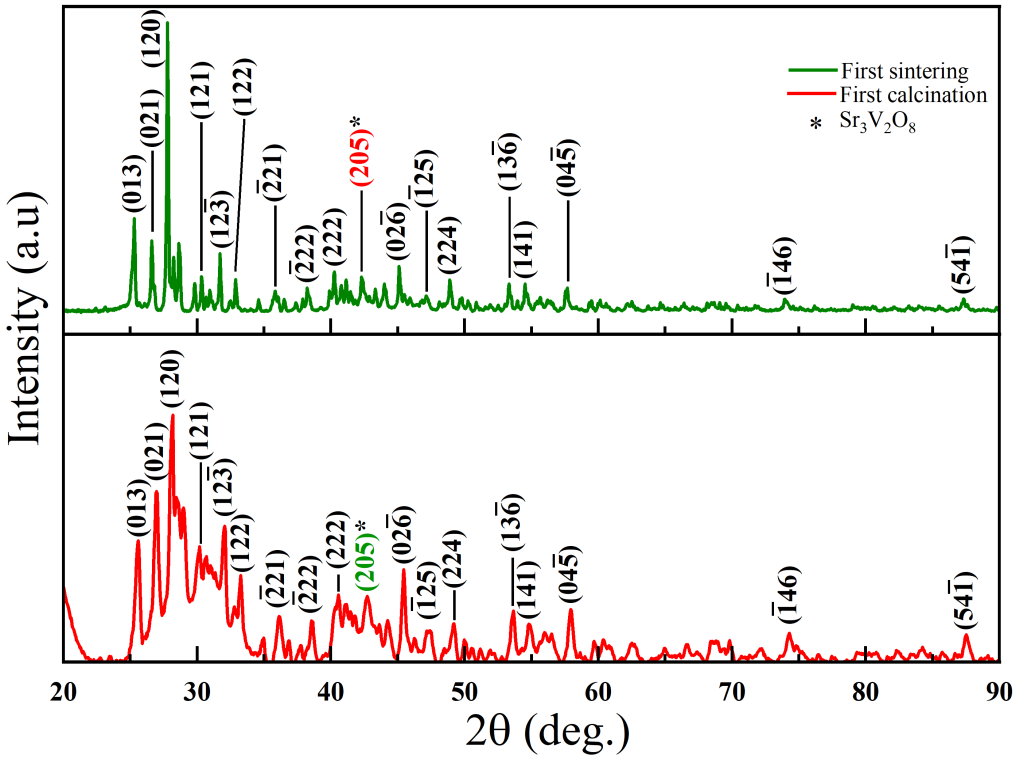

Figure 14: XRD graphs of $Sr_2V_2O_7$ pre-calcination (bottom) and post-calcination (top) where the asterisk is used to denote the secondary phase, $Sr_3V_2O_8$.

Characterizing the XRD for $Sr_2V_2O_7$ was difficult due to the numerous peaks both of high and low intensity, especially since it was determined that the secondary phase $Sr_3V_2O_8$ peaks were also found. $Sr_3V_2O_8$ has a triagonal crystal structure meaning that only two lengths of the three match and two angles are 90°while the other is 120°, this crystal structure still results in numerous peaks as well. Additionally, $Sr_3V_2O_8$ has similar peaks to $Sr_2V_2O_7$ which made characterizing the XRD graph more difficult. As indicated by Figure 14, the current sample still retains some of the other phase, this is not concerning as the presence of it is few and there having been experiments conducted with $SrVO_3$ with only 85% $SrVO_3$ and 15% of its secondary phase [7].

3.2 Atomic Force Microscopy (AFM)

AFM is a type of scanning probe microscopy with a extremely high resolution, the AFM machine used is shown in Figure 15. It has a demonstrated resolution on the order of fractions of a nanometer, making it more than 1000 times better than the optical diffraction limit.

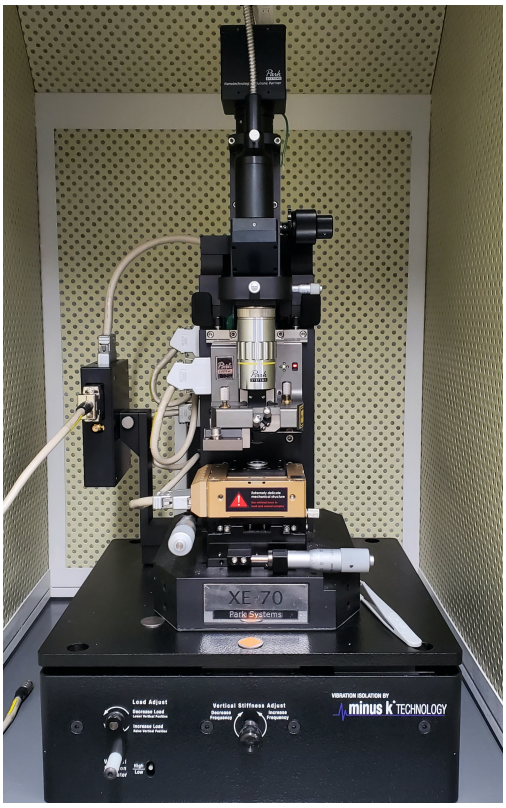

Figure 15: AFM machine

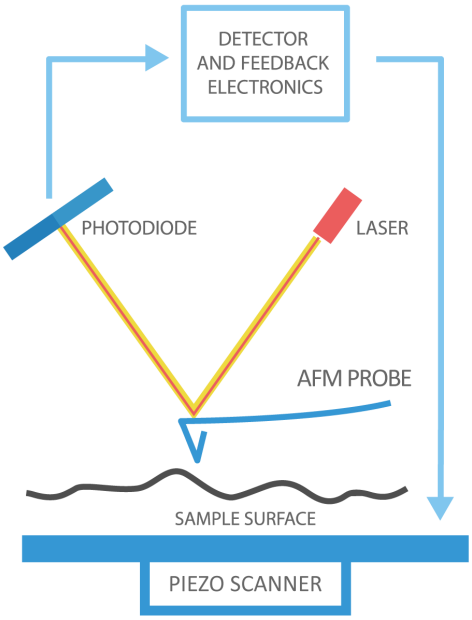

Figure 16: AFM diagram

By probing the surface of the sample with a tip, information about the sample can be collected, that information, for this experiment, being the topographic image of the sample as seen by Figure 16.

3.3 Pulse Laser Deposition (PLD)

Pulse Laser Deposition is a technique used to prepare thin films by irradiating a target, thus creating a plasma plume as demonstrated by Figure 17. The plume expands outwards towards the substrate, where then the target material is deposited on it, this deposition is what creates the thin film. When perovskites are structured in layers using techniques like PLD, new types of interesting properties are exhibited by the thin films. These interesting properties include colossal magnetoresistance, ferroelectricity, superconductivity, charge ordering, spin dependent transport, high thermopower, etc. [9].

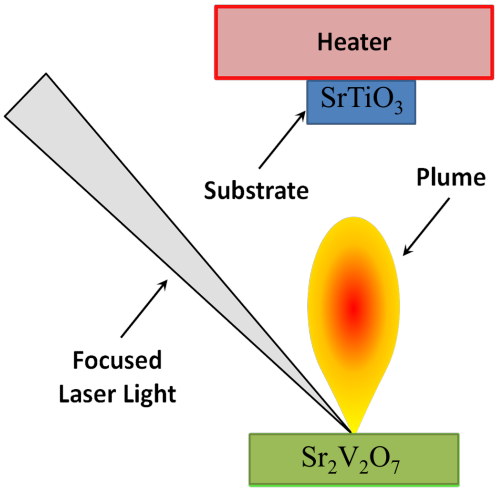

Figure 17: PLD diagram

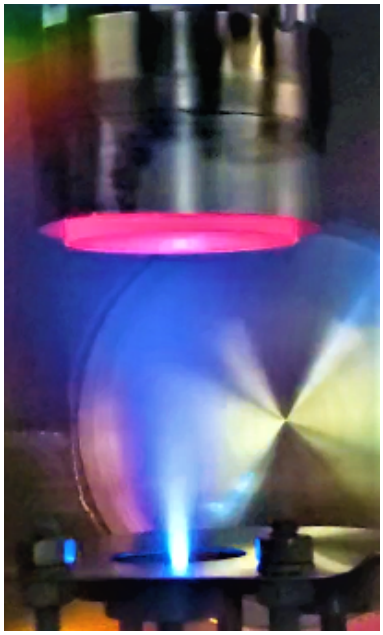

Figure 18: $SrVO_3/SrTiO_3$ thin film grown using PLD

The $SrVO_3$ (SVO) thin film was deposited using PLD on a (001)-oriented $SrTiO_3$ (STO) substrate as seen in Figure 18. Before deposition was done, the surface of the target was laser cleaned for 5 minutes. The thin film was deposited at 750 °C with 10 mtorr O_2 for 40 minutes with 467 mJ of energy. While the $Sr_2V_2O_7$ target has an excess of oxygen, the 10 mtorr of O_2 is used to slow down the plume for better growth. XRD was used to determine if $SrVO_3$ had successfully deposited onto $SrTiO_3$ [10]. Looking at Figure 19, it was expected for the highest intensity peaks to be $SrTiO_3$ due to the thin film only having a thin layer of $SrVO_3$ and the rest being $SrTiO_3$. It was determined that there are $SrVO_3$ and $Sr_2V_2O_7$ peaks, indicating that while the deposition was successful, the quality was poor.

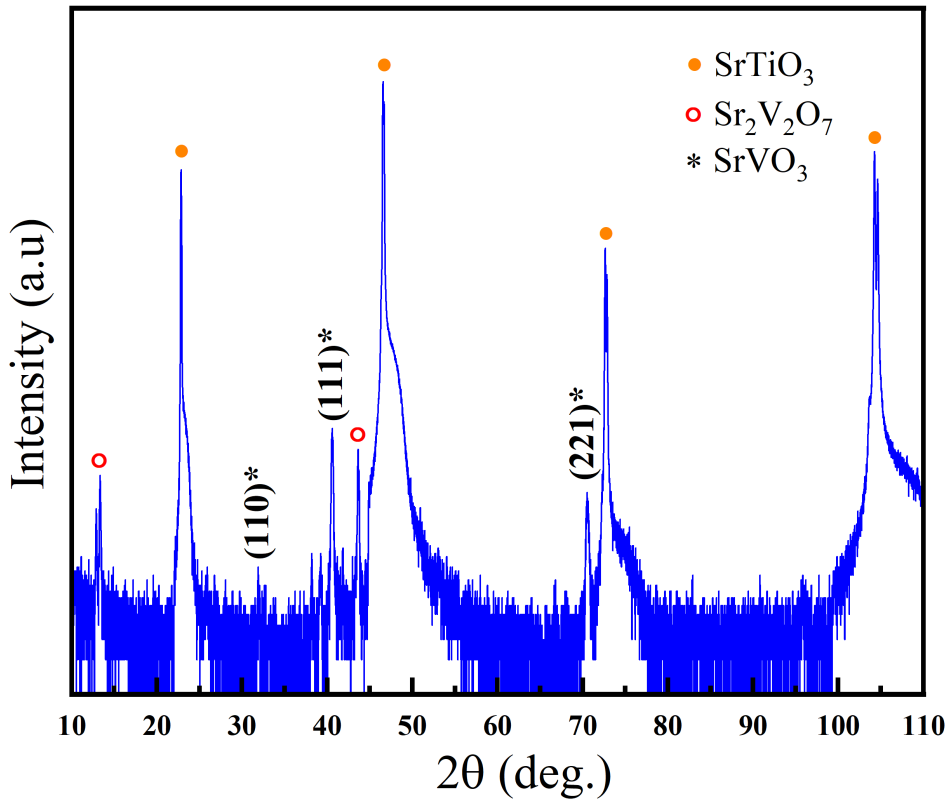

Figure 19: XRD graph of the $SrVO_3/SrTiO_3$ thin film

4 Conclusion

Despite $Sr_2V_2O_7$ being a secondary phase of $SrVO_3$, the thin film was determined to have $SrVO_3$ peaks indicating that $SrVO_3$ was successfully grown on $SrTiO_3$. For future work, the $Sr_2V_2O_7$ could be better synthesized to further reduce other secondary phases from appearing and to yield a better quality $SrVO_3$ thin film, and instead of using 10 mtorr of O_2, the deposition can be done in a vacuum, or with less O_2. The overall growth conditions should be better optimized to grow higher quality $SrVO_3$ thin films. Furthermore, instead of using $Sr_2V_2O_7$ as the target, $SrVO_3$ could be synthesized and used as the target.

Acknowledgments

I want to express my appreciation towards my mentor Dr. Ambrose Seo and the graduate student Sujan Shrestha for the assistance and meaningful discussions and feedback throughout the program. Thanks to them I have acquired different experimental skills and learned new techniques.

I want thank W. J. Gannon and his students, B. Arnold and S. Bhusal, for their assistance and the use of their furnace. I also want to thank L. DeLong for providing and allowing use of the die set and dry press and N. Miller for usage of the x-ray diffractor. This research was supported by the National Science Foundation grant DMR-2104296 and PHY-1950795.

References

[1] R. Xu, et al. ACS Appl. Mater. Interfaces 12, 16462-16468 (2020).

[2] G. Wang, et al. Phys. Rev. B 100, 155114 (2019).

[3] M. Brahlek, et al. MRS Communications 7, 27-52 (2017).

[4] M. Verma and R. Pentcheva, Phys. Rev. Research 4, 033013 (2022).

[5] Y. Okada, et al. Phys. Rev. Lett. 119, 086801 (2017).

[6] M. Onada, H. Ohta, H. Nagasawa, Solid State Commun. 79, 281-285 (1991).

[7] T. Berry, et al. Journal of Crystal Growth 583, 126518 (2022).

[8] J. G. Connell, et al. Appl. Phys Lett. 101, 251607 (2012).

[9] J. Wang, G. Rijnders, G. Koster, Appl. Phys. Lett. 113, 223103 (2018).

[10] T. Maekawa, K. Kurosaki, S. Yamanaka, Journal of Alloys and Compounds 426, 46-50 (2006).